Multiorbital impact on strong-field ionization of HCl molecules

Shilin Hu,[1,*] Zheng Shu,[2] Li Guo,[3,†] and Jing Chen[2,4,‡]

[1]*Guangdong Provincial Key Laboratory of Quantum Metrology and Sensing and School of Physics and Astronomy, Sun Yat-Sen University (Zhuhai Campus), Zhuhai 519082, China*

[2]*Institute of Applied Physics and Computational Mathematics, P. O. Box 8090, Beijing, 100088, China*

[3]*Department of Physics, Shanghai Normal University, Shanghai 200234, China*

[4]*Shenzhen Key Laboratory of Ultraintense Laser and Advanced Material Technology, Center for Advanced Material Diagnostic Technology, and College of Engineering Physics, Shenzhen Technology University, Shenzhen 518118, China*

(Received 16 June 2021; accepted 30 September 2021; published 25 October 2021)

We have put forward the time-dependent Hartree-Fock approach to investigate ionization dynamics of HCl molecules subjected to strong few-cycle laser pulses, which is based on the finite-element discrete-variable representation in prolate spheroidal coordinates and the Crank-Nicolson method. It is demonstrated that the electron is favored to be freed by the peak electric field pointing towards the H atom for the HCl molecule possessing the bonding length $R = 2.5$ a.u., while the ionization prefers to occur for the maximum electric field pointing from the H nucleus to Cl nucleus with increasing internuclear separations. Analysis indicates that the ionization yield of 5σ electrons becomes significant with respect to that of 2π electrons with stretching bonding lengths, and the relative contributions of the ionization from 5σ and 2π electrons change as a function of internuclear separations, which gives rise to the above distinct oriented ionization of HCl molecules.

DOI: 10.1103/PhysRevA.104.043110

I. INTRODUCTION

Strong-field ionization is considered as the starting point when an intense laser pulse interacts with atoms and molecules and a trigger for subsequent dynamic processes of significant current interest, such as high-order harmonic generation (HHG) [1–4], frustrated tunneling ionization [5–7], laser-induced electron diffraction [8,9], and Coulomb explosion [10–12], which are helpful for comprehending strong-field molecular physics and developing techniques for ultrafast imaging of molecular structures. Compared with atoms, the ionization behavior of molecules subjected to an intense laser field is much more complicated due to the additional nuclear degrees of freedom. For example, anomalously high ionization of molecules takes place when the molecules are stretched to some critical bond lengths for orientations parallel to the linearly polarized laser fields [13–15]. The ionization yields of diatomic molecules show oscillatory behavior as a function of internuclear separations and alignment angles in intense laser pulses [16,17], and the oscillation shows strong dependence on the molecular structures [18], which is attributed to the distinct interferences of the subwaves of the emitted electron emerging from different atomic sites.

Since the impact of subcycle modifications of the electric field on molecular processes is of significant interest for achievements of coherent control and applications of charged-directed chemical reactions, the manipulation of electron dynamics for different molecules in few-cycle laser pulses has attracted great attention recently. The electron localization on one of the dissociating nuclei can be controlled by adjusting the carrier-envelope phase (CEP) of the near-infrared pulse when H_2^+ molecules are subjected to few-cycle laser pulses [19]. The directional emission of D^+ fragments from the dissociative ionization of complex multielectron DCl molecules can be achieved by changing the CEP of few-cycle laser pulses [20,21]. For CO molecules multiple dissociative ionization channels can also be selectively steered by altering the CEP of intense few-cycle pulses [22].

More recently, when high-performance experimental technologies for orienting molecules became available, strong interest has been directed towards the study of oriented molecular ionization in experimental and theoretical research. The experimental observation of orientation-dependent ionization of N_2 and O_2 molecules is consistent with the molecular Ammosov-Delone-Krainov (MO-ADK) calculations, which are based on single-active-electron (SAE) approximations, while the narrow ionization distribution of CO_2 molecules and its peak ionization at alignment angle 45° deviate from the above SAE simulations [23,24], and improvements of the asymptotic wave function, multiorbital effects, and dynamic exchange roles have been put forward to resolve discrepancies between experimental data and theoretical results for the ionization behavior of CO_2 molecules [25–27]. For CO molecules, it is demonstrated that higher ionization yields occur when the molecule is oriented with the electric field pointing from C end to O end in experiments [28]. The above finding is different from the prediction based on the calculations of the time-dependent Schrödinger equation (TDSE)

*hushlin@mail.sysu.edu.cn
†guoli@shnu.edu.cn
‡chen_jing@iapcm.ac.cn

within SAE approximations [29], while the multielectron dynamics plays a vital role in the anisotropic ionization of CO molecules in recent theoretical studies [30–32], and the experimental studies of ionization dynamics of CO molecules also reveals that the electrons in low-lying orbitals contribute to the ionization [33,34]. It becomes evident that the improvements of theoretical simulations adopting SAE approximation to study the ionization dynamics of multielectron molecules are needed.

In theory, time-dependent density-functional theory (TDDFT) and the multiconfiguration time-dependent Hartree-Fock theory (MCTDHF) are proposed to describe the multielectron effects on molecular ionization. The TDDFT calculations show dependence on the formulas of the exchange-correlation potential [35–37], while the computation of MCTDHF is extremely demanding [38,39]. In addition, the time-dependent Hartree-Fock (TDHF) theory has attracted great attention, because the computation is affordable for complex systems and the interactions of all electrons with strong laser fields can be taken into account. The difference between MCTDHF and TDHF is that the total wave function is expanded in terms of many Slater determinants with time-varying molecular orbitals and coefficients, and the quantitative accuracy of the description on the correlated electron motion can be greatly improved with the increasing expansion lengths for MCTDHF. For TDHF, the multielectron wave function is approximated by a single Slater determinant, and the molecular orbitals involved are propagated based on the mean field approximation, so TDHF is the simplest version of the MCTDHF scheme. TDHF has been employed to investigate the enhanced ionization of C_2H_2 molecules exposed to strong laser fields [40,41], and the existence of a multiple-bond version of enhanced ionization in polyatomic molecules is consistent with the experimental observations [42,43]. The TDHF approach has been adopted to study the alignment-dependent ionization of CO molecules in an intense laser field, the results are in good agreement with the experimental findings [33], and the analysis indicates that the dynamic core polarization has an important impact on the strong-field molecular ionization [44]. More recently, it has been found that inner-orbital electron dynamics plays a vital role in the ionization of C_2H_2 molecules and the HHG of CO molecules in intense laser fields based on TDHF calculations [45,46].

As stated above, multielectron dynamics plays a vital role in the ionization of molecules exposed to strong laser pulses [26,27,33,34,44,47,48], and directional emission of fragments from the dissociative ionization of complex multielectron polar molecules can be controlled with few-cycle laser pulses [20–22], while the study of the oriented ionization of multielectron polar molecules with different internuclear separations is rare, which is helpful for further understanding the aforementioned experimental observations. In this work, the oriented ionization of HCl molecules possessing different bonding lengths in few-cycle laser pulses has been studied with TDHF, in which finite-element discrete-variable representation (FEDVR) and the Crank-Nicolson approach are used. It is demonstrated that the electron tends to be detached by the peak electric field pointing towards H atom for a HCl molecule with the internuclear separation $R = 2.5$ a.u., while the ionization is more likely to take place if the maximum electric field points from the H end to Cl end with increasing bonding lengths, and the above peculiar ionization behaviors stem from the change of relative contributions of the ionization from 5σ and 2π electrons with stretching bonding lengths. Atomic units (a.u.) are employed unless otherwise indicated.

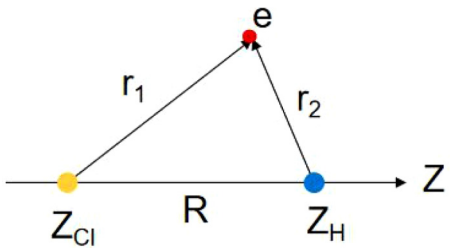

FIG. 1. Coordinates of HCl molecule.

II. THEORETICAL APPROACHES

Within the dipole approximation and fixed nuclear approximation, the TDHF equations of HCl molecules subjected to the strong laser pulses read as [41,45]

$$i\frac{\partial}{\partial t}\Psi_i(\mathbf{r},t)=[H_1(\mathbf{r})+2J(\mathbf{r},t)-K(\mathbf{r},t)+\mathbf{r}\cdot\mathbf{E}(t)]\Psi_i(\mathbf{r},t). \tag{1}$$

In order to study the dynamics of diatomic molecule HCl in laser fields, it is natural to choose prolate spheroidal coordinates to present the electron. r_1 and r_2 represent the separations from the two nuclei, and R indicates the bonding length in Fig. 1. We then define $\xi=(r_1+r_2)/R$, $\eta=(r_1-r_2)/R$, and the azimuthal angle φ. The one-electron Hamiltonian of H_1(r) is given by

$$H_1(\mathbf{r}) = -\frac{2}{R^2(\xi^2-\eta^2)}\left[\frac{\partial}{\partial\xi}(\xi^2-1)\frac{\partial}{\partial\xi}+\frac{\partial}{\partial\eta}(1-\eta^2)\frac{\partial}{\partial\eta}+\frac{\xi^2-\eta^2}{(\xi^2-1)(1-\eta^2)}\frac{\partial^2}{\partial\varphi^2}\right]-\frac{2}{R}\left[\frac{Z_H}{\xi+\eta}+\frac{Z_{Cl}}{\xi-\eta}\right], \tag{2}$$

where $Z_{Cl}=17$ and $Z_H=1$ denote the charges of Cl nucleus and H nucleus, respectively. $J(r,t)$ and $K(r,t)$ represent electron-electron Coulomb interaction and electron-electron exchange interaction, respectively,

$$J(\mathbf{r}_1,t)\Psi_i(\mathbf{r}_1,t)=\sum_j^N\int\frac{|\Psi_j(\mathbf{r}_2,t)|^2}{\mathbf{r}_{12}}d\mathbf{r}_2\Psi_i(\mathbf{r}_1,t) \tag{3}$$

and

$$K(\mathbf{r}_1,t)\Psi_i(\mathbf{r}_1,t)=\sum_j^N\int\frac{\Psi_j^*(\mathbf{r}_2,t)\Psi_i(\mathbf{r}_2,t)}{\mathbf{r}_{12}}d\mathbf{r}_2\Psi_j(\mathbf{r}_1,t), \tag{4}$$

where N denotes the number of occupied orbitals. Two-electron interaction operator is expressed as

$$\frac{1}{r_{12}}=\frac{2}{R}\sum_{l=0}^{\infty}\sum_{m=-l}^{l}(-1)^{|m|}(2l+1)\left(\frac{(l-|m|)!}{(l+|m|)!}\right)^2P_l^{|m|}(\xi_<)\times Q_l^{|m|}(\xi_>)P_l^{|m|}(\eta_1)P_l^{|m|}(\eta_2)e^{im(\varphi_1-\varphi_2)}, \tag{5}$$

where $\xi_<$ and $\xi_>$ correspond to min(max)(ξ_1, ξ_2), and $P_l^{|m|}(\xi_<)$ and $Q_l^{|m|}(\xi_>)$ indicate regular and irregular Legendre functions, respectively.

As stated above, the electron-electron interactions are time-varying in TDHF theory, so highly efficient calculations of two-electron integrals are required. It has been confirmed that the FEDVR is high-performance and accurate in carrying out two-electron integral calculations [39,44,45], so the time-dependent wave functions can be expanded by FEDVR as follows:

$$\Psi_i(\xi, \eta, \varphi, t) = \frac{1}{\sqrt{2\pi}}\left(\frac{2}{R}\right)^{\frac{3}{2}} \sum_{\mu\nu} C_{\mu\nu}(t) f_\mu(\xi) g_\nu(\eta) e^{im\varphi}. \quad (6)$$

For even $|m|$, the DVR basis is given by

$$f_\mu(\xi) = \frac{1}{\sqrt{\omega_\xi^\mu}} \prod_{k\neq\mu} \frac{\xi - \xi_k}{\xi_\mu - \xi_k}, \; g_\nu(\eta) = \frac{1}{\sqrt{\omega_\eta^\nu}} \prod_{k\neq\nu} \frac{\eta - \eta_k}{\eta_\nu - \eta_k}. \quad (7)$$

In order to properly describe the nonanalytic behavior of the wave functions near the boundaries of $\xi = 1$ and $\eta = \pm 1$ for odd $|m|$, the DVR basis of odd $|m|$ is defined as [49]

$$f_\mu(\xi) = \frac{1}{\sqrt{\omega_\xi^\mu}} \frac{(\xi^2-1)^{1/2}}{\left(\xi_\mu^2-1\right)^{1/2}} \prod_{k\neq\mu} \frac{\xi - \xi_k}{\xi_\mu - \xi_k},$$

$$g_\nu(\eta) = \frac{1}{\sqrt{\omega_\eta^\nu}} \frac{(\eta^2-1)^{1/2}}{\left(\eta_\nu^2-1\right)^{1/2}} \prod_{k\neq\nu} \frac{\eta - \eta_k}{\eta_\nu - \eta_k}. \quad (8)$$

Gauss-Radau quadrature points ξ_μ are adopted in the first DVR element in the ξ direction, Gauss-Lobatto quadrature points ξ_μ are used in other elements, and Gauss-Legendre quadrature points η_ν are employed in the η direction. The two-electron integrals are obtained by solving Poissons equations, and the details can be found in Ref. [49]. The details of molecular Hartree-Fock calculations can be found in our previous work [50]. The time-varying wave functions are propagated with the Crank-Nicolson approach in this work [45], which is different from the time propagation method of iterative Lanczos algorithm in the previous TDHF method [44,51], since the Crank-Nicolson approach is stable and accurate [52], and orthogonality of different orbitals is enforced during the time evolution. A $\cos^{1/8}$ absorber function is employed in the range $[2\xi_{\max}/3, \xi_{\max}]$ to avoid unphysical reflection of the electron wave packet from the boundary. The time-varying wave functions are propagated long enough to allow all the ionization flux to pass through the absorbing boundary after the conclusion of the strong laser pulse, and then the ionization probability of the i orbital is defined as $P_i(t_{\text{end}}) = 1 - \langle\Psi_i(\mathbf{r}, t_{\text{end}})|\Psi_i(\mathbf{r}, t_{\text{end}})\rangle$. The total ionization probability is given by $P_t = 1 - \prod_i (1 - P_i)$. The component of the α field-free orbital contained by the β time-varying orbital is written as $P_{\alpha\beta}(t) = |\langle\Psi_\alpha(\mathbf{r}, t = 0)|\Psi_\beta(\mathbf{r}, t)\rangle|^2$.

In this paper, $\xi_{\max}$=150/R a.u. is adopted, and 160 and 30 FEDVR bases are employed in the ξ and η directions, respectively. The laser fields are parallel to the molecular axis, the vector potential is written as $\mathbf{A}(t) = \frac{E_0}{\omega} \sin^2(\pi t/t_{\max}) \sin(\omega t + \theta)\hat{z}$ $(0 < t < t_{\max})$ with carrier envelope phase (CEP) θ, and the time-varying electric field is defined as $\mathbf{E}(t) = -\partial\mathbf{A}(t)/\partial t$. E_0, $t_{\max}$, and ω indicate the peak electric field, the duration, and the angular frequency, respectively. The total pulse duration is three optical cycles with the wavelength $\lambda = 800$ nm ($\omega = 0.057$ a.u.), and the time step is $\Delta t = 0.03$ a.u. Convergence of numerical simulations is achieved with the above settings.

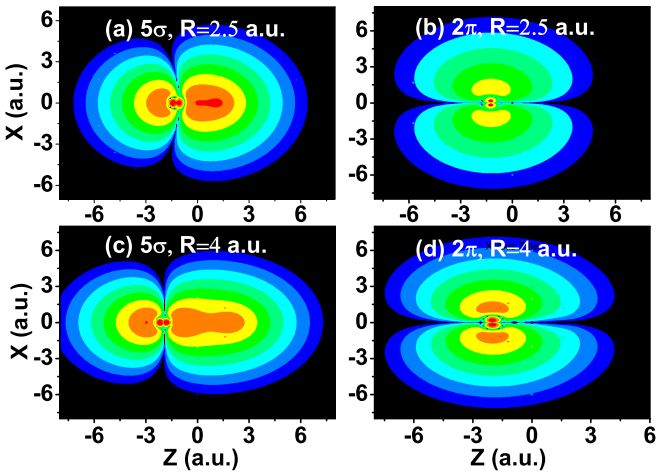

FIG. 2. Orbital densities of HCl molecules with different bonding lengths. (a) 5σ orbital ($R = 2.5$ a.u.), (b) 2π orbital ($R = 2.5$ a.u.), (c) 5σ orbital ($R = 4$ a.u.), and (d) 2π orbital ($R = 4$ a.u.).

III. RESULTS AND DISCUSSIONS

The orbital energies of HCl molecules are displayed in Table I, and the reference values are calculated with aug-cc-pvqz basis sets at the Hartree-Fock level [53]. It is found that our results agree well with the reference and experimental data [53,54]. The charge distributions of different orbitals for HCl molecules with different bonding lengths are plotted in Fig. 2, and the origin locates the midpoint between the Cl nucleus and the H nucleus. It is shown that the orbital densities of 5σ orbital are distributed along the molecular axis, while the charge distributions of 2π orbital are away from the molecular axis. Figure 3 depicts the field-free orbital energies ε_i with the increase of internuclear separations R, and the orbital energies of 1σ, 2σ, 3σ, and 1π are not shown due to their lower energies with respect to those of 4σ, 5σ, and 2π electrons. It is worthwhile to mention that the orbital energies of 5σ are close to those of 2π near $R = 4$ a.u., and the gaps

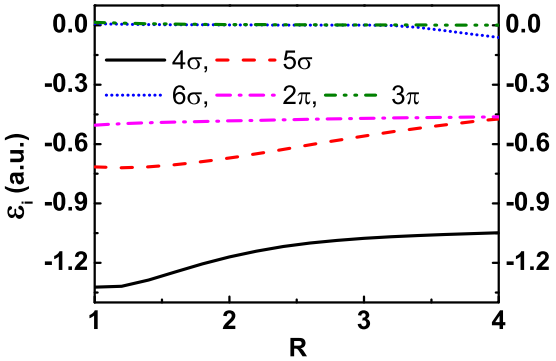

FIG. 3. Field-free orbital energies ε_i as a function of internuclear distances R.

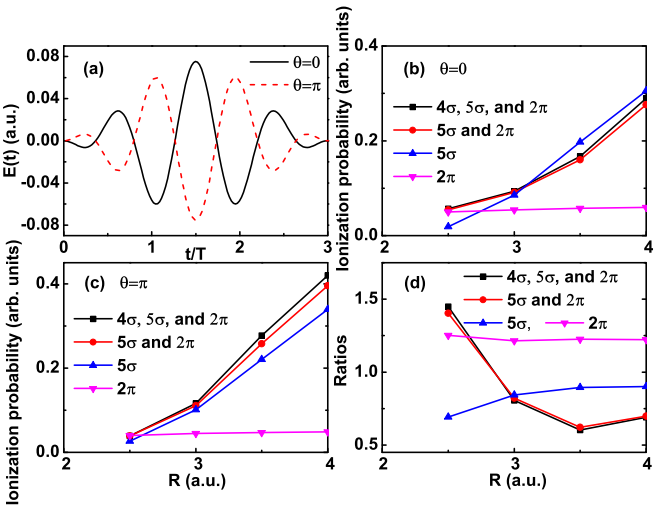

FIG. 4. (a) The time-dependent electric field of CEP $\theta = 0$, π and laser intensity 200 TW/cm^2 ($T = 2\pi/\omega$). (b) Ionization probabilities obtained by time propagating three orbitals (4σ, 5σ, and 2π), two orbitals (5σ and 2π), and one orbital (5σ or 2π) for CEP $\theta = 0$. (c) Same as (b) but for CEP $\theta = \pi$. (d) Ratios of $P_t(\theta = 0)/P_t(\theta = \pi)$ obtained by propagating three orbitals (4σ, 5σ, and 2π), two orbitals (5σ and 2π), and one orbital (5σ or 2π) in the corresponding panels (b) and (c).

between 5σ orbital energies and 6σ orbital energies become narrower with increasing bonding lengths R.

Figure 4(a) depicts the time-dependent electric fields corresponding to the laser pulses of the intensity 200 TW/cm^2 and CEP $\theta = 0$ or π. The maximum electric field points from the Cl end to H end in the HCl molecule for $\theta = 0$, and the peak electric field points from the H nucleus to Cl nucleus for $\theta = \pi$ in Fig. 1. The ionization energies of 1σ, 2σ, 3σ, and 1π electrons are much higher compared with those of electrons in other orbitals in Table I, so 1σ, 2σ, 3σ, and 1π orbitals keep frozen in the time propagation of TDHF equations. Figures 4(b) and 4(c) show the ionization yields obtained by time propagating three orbitals (4σ, 5σ, and 2π), two orbitals (5σ and 2π), and one orbital (5σ or 2π) in Eq. (1) with increasing bonding lengths for CEP $\theta = 0$ and $\theta = \pi$, respectively, while electrons in other shells are frozen. It is found that the simulations adopting two orbitals (5σ and 2π) are close to those employing three orbitals (4σ, 5σ, and 2π), and the role of 4σ electrons dynamics in the ionization yields

TABLE I. Comparison of orbital energies (a.u.) of HCl molecules with $R = 2.5$ a.u. calculated with field-free molecular Hartree-Fock methods and experimental data.

Orbitals	Present	[53]	Exp. [54]
1σ	−104.84271	−104.85143	
2σ	−10.57581	−10.57567	
3σ	−8.04141	−8.04273	
1π	−8.04129	−8.04116	
4σ	−1.10826	−1.10856	
5σ	−0.61551	−0.61545	−0.599
2π	−0.47585	−0.47587	−0.471

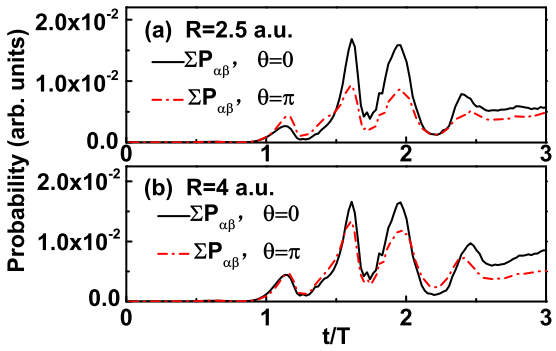

FIG. 5. The sum of probabilities of field-free unoccupied π orbitals in time-dependent $\Psi_{2\pi}(\mathbf{r}, t)$ obtained by time propagating only the 2π orbital in TDHF calculations for HCl molecules possessing different bonding lengths in few-cycle laser pulses with CEP $\theta = 0$ or π ($T = 2\pi/\omega$). (a) $R = 2.5$ a.u. and CEP $\theta = 0$ or π, (b) $R = 4$ a.u. and CEP $\theta = 0$ or π. For visual convenience, the time-varying probabilities of 2π are not depicted.

is negligible due to its large ionization energies with respect to those of 5σ and 2π electrons in Fig. 3. In addition, it is demonstrated that, as the bonding lengths are stretched, the ionization probabilities of 5σ electrons increase significantly, while the ionization yields of 2π electrons change slightly compared with those of 5σ electrons for the TDHF calculations by time propagating one orbital (5σ or 2π).

In order to clearly show the discrepancies of ionization yields for CEP between $\theta = 0$ and $\theta = \pi$, ratios of $P_t(\theta = 0)/P_t(\theta = \pi)$ are depicted in Fig. 4(d), which are calculated by propagating three orbitals (4σ, 5σ, and 2π), two orbitals (5σ and 2π), and one orbital (5σ or 2π) in Figs. 4(b) and 4(c). It is found that the ratio of $P_t(\theta = 0)/P_t(\theta = \pi)$ is larger than 1 at $R = 2.5$ a.u. in TDHF simulations by time propagating three orbitals (4σ, 5σ, and 2π) and two orbitals (5σ and 2π), which indicates that electrons tend to be detached when the peak electric field points from Cl nucleus to H nucleus. However, as the internuclear separations are stretched further, the ratios of $P_t(\theta = 0)/P_t(\theta = \pi)$ are smaller than 1 for TDHF calculations by time propagating three orbitals (4σ, 5σ, and 2π) and two orbitals (5σ and 2π), which denotes that electrons are more likely to be freed by the peak electric field pointing from H end to Cl end. The ratios of $P_t(\theta = 0)/P_t(\theta = \pi)$ are smaller than 1 by time evolution of the 5σ orbital in TDHF simulations, so the molecular ionization tends to occur if the peak electric field points towards Cl atom for taking into account only the interactions of laser pulses and 5σ electrons. The ratios of $P_t(\theta = 0)/P_t(\theta = \pi)$ are larger than one by only time propagating the 2π orbital, which indicates that the electrons are more probable to be detached by the peak electric field pointing towards the H end if only 2π orbital is time evolution in TDHF calculations.

To further understand the distinct ionization behaviors of HCl molecules in few-cycle laser pulses in Fig. 4, we display the sum of the time-varying probabilities $P_\alpha(t)$ of unoccupied orbitals π in time-dependent $\Psi_{2\pi}(\mathbf{r}, t)$ for HCl molecules possessing $R = 2.5$ a.u. and $R = 4$ a.u. when only the 2π orbital is time propagating in TDHF calculations with other orbitals being frozen in Fig. 5 (α indicates the time-independent

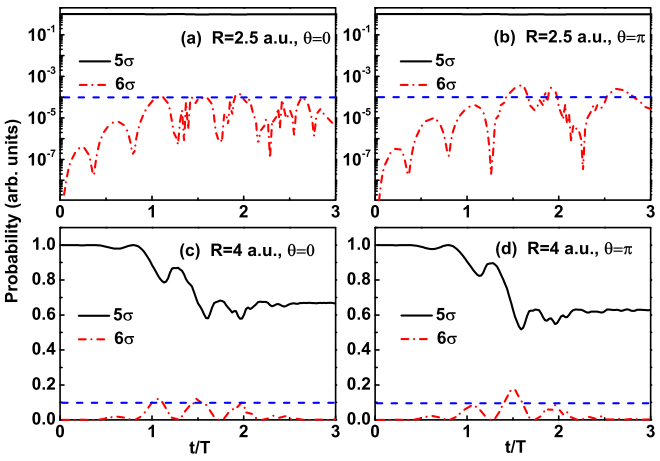

FIG. 6. Time-dependent probabilities of 5σ and 6σ orbitals are calculated by time propagating only the 5σ orbital in TDHF calculations (other orbitals keep frozen) for HCl molecules possessing different bonding lengths in few-cycle laser pulses of CEP $\theta = 0$ or π ($T = 2\pi/\omega$). (a) $R = 2.5$ a.u. and CEP $\theta = 0$, (b) $R = 2.5$ a.u. and CEP $\theta = \pi$, (c) $R = 4$ a.u. and CEP $\theta = 0$, (d) $R = 4$ a.u. and CEP $\theta = \pi$. Blue dash lines are added for visual convenience.

unoccupied π orbitals, which range from the first unoccupied orbital to the 50th unoccupied orbital). For visual convenience, the time-dependent probabilities of 2π are not plotted, since the probabilities of 2π are much larger with respect to those of other unoccupied orbitals. It is found that the mixings of 2π and other occupied orbitals are obviously stronger for CEP $\theta = 0$ than those corresponding to CEP $\theta = \pi$ for HCl molecule at the internuclear distance $R = 2.5$ a.u. and $R = 4$ a.u. in Fig. 5, which leads to the fact that the ratio of $\mathrm{P}_t(\theta = 0)/P_t(\theta = \pi)$ is larger than 1 for $R = 2.5$ a.u. and $R = 4$ a.u. when only the 2π orbital is taken into account in time evolution of TDHF simulations in Fig. 4(d).

In Fig. 6 we show the components of time-independent orbitals 5σ and 6σ in time-varying orbital $\Psi_{5\sigma}(\mathbf{r}, t)$ for HCl molecules with different internuclear separations subjected to few-cycle laser pulses of different CEPs, which are obtained by the time evolution of only the 5σ orbital in TDHF simulations and keeping other orbitals frozen. It is demonstrated that the coupling between 5σ and the unoccupied molecular orbital 6σ becomes stronger with increasing bonding lengths for the same CEP due to narrower energy gaps for 5σ and 6σ orbitals in Fig. 3 ($< \Psi_{5\sigma}(\mathbf{r}, t = 0)|Z|\Psi_{6\sigma}(\mathbf{r}, t = 0) >= 0.04$ for the energy gap 0.616 a.u. between 5σ and 6σ state at $R = 2.5$ a.u. and $< \Psi_{5\sigma}(\mathbf{r}, t = 0)|Z|\Psi_{6\sigma}(\mathbf{r}, t = 0) >= -1.93$ for the energy gap 0.411 a.u. between the 5σ and 6σ state at $R = 4$ a.u.), which accounts for the significant increase of ionization yields of 5σ electrons with increasing internuclear distances compared with the ionization yields of 2π electrons vs bonding lengths in Fig. 4. For the same bonding length, there is stronger mixing between 5σ and 6σ orbitals for CEP $\theta = \pi$ with respect to that for CEP θ=0, so the the ratios of $\mathrm{P}_t(\theta = 0)/P_t(\theta = \pi)$ are smaller than one by only time propagating the 5σ orbital in Fig. 4(d).

At $R = 2.5$ a.u., the total ionization is mainly determined by 2π electron dynamics due to its lower ionization energy compared with those of electrons in other shells in Table I, and the mixings between the 2π orbital and other unoccupied orbitals are stronger for CEP $\theta = 0$ with respect to those for CEP $\theta = \pi$, so the ratios of $\mathrm{P}_t(\theta = 0)/P_t(\theta = \pi)$ are larger than one for the time propagation of TDHF equations adopting three orbitals (4σ, 5σ, and 2π) and two orbitals (5σ and 2π) in Fig. 4(d). As the bonding lengths are stretched, the ionization energy of 5σ electrons become smaller in Fig. 3, and the coupling between the 5σ orbital and the unoccupied molecular orbital 6σ becomes stronger for CEP $\theta = \pi$ compared with that for CEP $\theta = 0$, so the ionization yields of the 5σ electrons are gradually dominant over those of electrons in other occupied orbitals, which gives rise to the fact that the ratios of $\mathrm{P}_t(\theta = 0)/P_t(\theta = \pi)$ calculated by time propagating three orbitals (4σ, 5σ, and 2π) and two orbitals (5σ and 2π) are smaller than 1 from $R = 3$ a.u. to $R = 4$ a.u. in Fig. 4(d). It is worthwhile to mention that we have studied the ionization dynamics of HCl molecules possessing the bonding lengths from 2.5 a.u. to 7 a.u. by time propagating three orbitals (4σ, 5σ, and 2π), which are subjected to the few-cycle laser pulse of the CEP $\theta = 0$ and the intensity 200 TW/cm^2, and the ionization probability increases with the stretched bonding lengths, so no enhanced ionization occurs for HCl molecules at the internuclear distance between 2 a.u. and 7 a.u. in our calculations. We do not investigate the ionization behaviors of HCl molecules with internuclear distance larger than 7 a.u., since the restricted Hartree-Fock methodology provides an inappropriate description of molecules at long bonding lengths [55].

IV. CONCLUSIONS

In summary, we have employed the TDHF method to study the ionization dynamics of HCl molecules possessing different bonding lengths in intense few-cycle laser pulses, and the FEDVR bases in prolate spheroidal coordinates and the Crank-Nicolson method are used in TDHF simulations. It is found that the ionization tends to take place when the peak electric field points from the Cl end to H end for the HCl molecule with internuclear distance $R = 2.5$ a.u., since the total ionization is mainly determined by the ionization of electrons in 2π orbital due to its lower ionization energy, and there exists evidently stronger coupling between 2π and other unoccupied molecular orbitals for the peak electric field pointing towards the H atom. As the bonding lengths are stretched, the mixing between the 5σ orbital and the unoccupied molecular orbital 6σ becomes more significant if the maximum electric field points towards Cl nucleus, and the ionization of 5σ electrons is dominant over that of electrons in other shells, so the electron is more likely to be detached for the peak electric field pointing from the H end to Cl end.

ACKNOWLEDGMENTS

This work was supported by the National Basic Research Program of China (Grants No. 2019YFA0307700 and No. 2016YFA0401100), the National Natural Science Foundation of China (Grants No. 11804405 and No. 11774361), the Key-Area Research and Development Program of Guangdong Province under Grant No. 2019B030330001, and the Science and Technology Program of Guangzhou (China) under Grant No. 201904020024.

[1] A. L'Huillier and Ph. Balcou, High-Order Harmonic Generation in Rare Gases with a 1-ps 1053-nm Laser, Phys. Rev. Lett. **70**, 774 (1993).

[2] P. B. Corkum, Plasma Perspective on Strong Field Multiphoton Ionization, Phys. Rev. Lett. **71**, 1994 (1993).

[3] K. J. Schafer, B. R. Yang, L. I. DiMauro, and K. C. Kulander, Above Threshold Ionization Beyond the High Harmonic Cutoff, Phys. Rev. Lett. **70**, 1599 (1993).

[4] F. Krausz and M. Ivanov, Attosecond physics, Rev. Mod. Phys. **81**, 163 (2009).

[5] B. B. Wang, X. F. Li, P. M. Fu, J. Chen, and J. Liu, Coulomb potential recapture effect in above-barrier ionization in laser pulses, Chin. Phys. Lett. **23**, 2729 (2006).

[6] T. Nubbemeyer, K. Gorling, A. Saenz, U. Eichmann, and W. Sandner, Strong-Field Tunneling Without Ionization, Phys. Rev. Lett. **101**, 233001 (2008).

[7] S. L. Hu, X. L. Hao, H. Lv, M. Q. Liu, T. X. Yang, H. F. Xu, M. X. Jin, D. J. Ding, Q. G. Li, W. D. Li, W. Becker, and J. Chen, Quantum dynamics of atomic Rydberg excitation in strong laser fields, Opt. Express **27**, 31629 (2019).

[8] M. Meckel, D. Comtois, D. Zeidler, A. Staudte, D. Pavičić, H. C. Bandulet, H. Pépin, J. C. Kieffer, R. Dörner, D. M. Villeneuve, and P. B. Corkum, Laser-induced electron tunneling and diffraction, Science **320**, 1478 (2008).

[9] C. I. Blaga, J. Xu, A. D. DiChiara, E. Sistrunk, K. Zhang, P. Agostini, T. A. Miller, L. F. DiMauro, and C. D. Lin, Imaging ultrafast molecular dynamics with laser-induced electron diffraction, Nature (London) **483**, 194 (2012).

[10] C. Cornaggia, M. Schmidt, and D. Normand, Coulomb explosion of CO_2 in an intense femtosecond laser field, J. Phys. B: At. Mol. Opt. Phys. **27**, L123 (1994).

[11] E. Baldit, S. Saugout, and C. Cornaggia, Coulomb explosion of N_2 using intense 10- and 40-fs laser pulses, Phys. Rev. A **71**, 021403(R) (2005).

[12] J. H. Posthumus, The dynamics of small molecules in intense laser fields, Rep. Prog. Phys. **67**, 623 (2004).

[13] T. Zuo and A. D. Bandrauk, Charge-resonance-enhanced ionization of diatomic molecular ions by intense lasers, Phys. Rev. A **52**, R2511 (1995).

[14] A. Saenz, Enhanced ionization of molecular hydrogen in very strong fields, Phys. Rev. A **61**, 051402(R) (2000).

[15] E. Constant, H. Stapelfeldt, and P. B. Corkum, Observation of Enhanced Ionization of Molecular Ions in Intense Laser Fields, Phys. Rev. Lett. **76**, 4140 (1996).

[16] S. Selstø, M. Førre, J. P. Hansen, and L. B. Madsen, Strong Orientation Effects in Ionization of H_2^+ by Short, Intense, High-Frequency Light Pulses, Phys. Rev. Lett. **95**, 093002 (2005).

[17] S. L. Hu, J. Chen, X. L. Hao, and W. D. Li, Effect of low-energy electron interference on strong-field molecular ionization, Phys. Rev. A **93**, 023424 (2016).

[18] S. L. Hu, M. Q. Liu, Z. Shu, and J. Chen, Impact of orbital symmetry on molecular ionization in an intense laser field, Phys. Rev. A **100**, 053414 (2019).

[19] F. He, C. Ruiz, and A. Becker, Control of Electron Excitation and Localization in the Dissociation of H_2 and Its Isotopes Using Two Sequential Ultrashort Laser Pulses, Phys. Rev. Lett. **99**, 083002 (2007).

[20] I. Znakovskaya, P. von den Hoff, N. Schirmel, G. Urbasch, S. Zherebtsov, B. Bergues, R. de Vivie-Riedle, K.-M. Weitzel, and M. F. Kling, Waveform control of orientation-dependent ionization of DCl in few-cycle laser fields, Phys. Chem. Chem. Phys. **13**, 8653 (2011).

[21] H. Li, X. M. Tong, N. Schirme, G. Urbasch, K. J. Betsch, S. Zherebtsov, F. Sümann, A. Kessel, S. A. Trushin, G. G. Paulus, K.-M. Weitzel, and M. F. Kling, Intensity dependence of the dissociative ionization of DCl in few-cycle laser fields, J. Phys. B: At. Mol. Opt. Phys. **49**, 015601 (2016).

[22] Y. Q. Liu, X. R. Liu, Y. K. Deng, C. Y. Wu, H. B. Jiang, and Q. H. Gong, Selective Steering of Molecular Multiple Dissociative Channels with Strong Few-Cycle Laser Pulses, Phys. Rev. Lett. **106**, 073004 (2011).

[23] D. Pavičić, K. F. Lee, D. M. Rayner, P. B. Corkum, and D. M. Villeneuve, Direct Measurement of the Angular Dependence of Ionization for N_2, O_2, and CO_2 in Intense Laser Fields, Phys. Rev. Lett. **98**, 243001 (2007).

[24] X. M. Tong, Z. X. Zhao, and C. D. Lin, Theory of molecular tunneling ionization, Phys. Rev. A **66**, 033402 (2002).

[25] S. F. Zhao, C. Jin, A. T. Le, T. F. Jiang, and C. D. Lin, Determination of structure parameters in strong-field tunneling ionization theory of molecules, Phys. Rev. A **81**, 033423 (2010).

[26] S. Petretti, Y. V. Vanne, A. Saenz, A. Castro, and P. Decleva, Alignment-Dependent Ionization of N_2, O_2, and CO_2 in Intense Laser Fields, Phys. Rev. Lett. **104**, 223001 (2010).

[27] V. P. Majety and A. Scrinzi, Dynamic Exchange in the Strong Field Ionization of Molecules, Phys. Rev. Lett. **115**, 103002 (2015).

[28] H. Li, D. Ray, S. De, I. Znakovskaya, W. Cao, G. Laurent, Z. Wang, M. F. Kling, A. T. Le, and C. L. Cocke, Orientation dependence of the ionization of CO and NO in an intense femtosecond two-color laser field, Phys. Rev. A **84**, 043429 (2011).

[29] M. Abu-samha and L. B. Madsen, Photoelectron angular distributions from polar molecules probed by intense femtosecond lasers, Phys. Rev. A **82**, 043413 (2010).

[30] S. Ohmura, T. Kato, T. Oyamada, S. Koseki, H. Ohmura, and H. Kono, A single-electron picture based on the multiconfiguration time-dependent Hartree-Fock method: Application to the anisotropic ionization and subsequent high-harmonic generation of the CO molecule, J. Phys. B: At. Mol. Opt. Phys. **51**, 034001 (2018).

[31] S. Ohmura, T. Kato, H. Ohmura, S. Koseki, and H. Kono, Analysis of the multielectron dynamics in intense laser-induced ionization of CO by the time-dependent effective potentials for natural orbitals, J. Phys. B: At. Mol. Opt. Phys. **53**, 184001 (2020).

[32] S. Ohmura, H. Ohmura, T. Kato, and H. Kono, Manipulation of multielectron dynamics of molecules by Fourier-synthesized intense laser pulses: Effective potential analysis of CO, Front. Phys. **9**, 677671 (2021).

[33] J. Wu, L. Ph. H. Schmidt, M. Kunitski, M. Meckel, S. Voss, H. Sann, H. Kim, T. Jahnke, A. Czasch, and R. Dörner, Multiorbital Tunneling Ionization of the CO Molecule, Phys. Rev. Lett. **108**, 183001 (2012).

[34] X. K. Li, J. Q. Yu, H. Y. Xu, X. T. Yu, Y. Z. Yang, Z. Z. Wang, P. Ma, C. C. Wang, F. M. Guo, Y. J. Yang, S. Z. Luo, and D. J. Ding, Multiorbital and excitation effects on dissociative double ionization of CO molecules in strong circularly polarized laser fields, Phys. Rev. A **100**, 013415 (2019).

[35] S. I. Chu, Recent development of self-interaction-free time-dependent density-functional theory for nonperturbative

treatment of atomic and molecular multiphoton processes in intense laser fields, J. Chem. Phys. **123**, 062207 (2005).

[36] E. P. Fowe and A. D. Bandrauk, Nonperturbative time-dependent density-functional theory of ionization and harmonic generation in OCS and CS_2 molecules with ultrashort intense laser pulses: Intensity and orientational effects, Phys. Rev. A **84**, 035402 (2011).

[37] P. Sándor, A. Sissay, F. Mauger, P. M. Abanador, T. T. Gorman, T. D. Scarborough, M. B. Gaarde, K. Lopata, K. J. Schafer, and R. R. Jones, Angle dependence of strong-field single and double ionization of carbonyl sulfide, Phys. Rev. A **98**, 043425 (2018).

[38] M. Kitzler, J. Zanghellini, Ch. Jungreuthmayer, M. Smits, A. Scrinzi, and T. Brabec, Ionization dynamics of extended multi-electron systems, Phys. Rev. A **70**, 041401(R) (2004).

[39] D. J. Haxton, K. V. Lawler, and C. W. McCurdy, Multiconfiguration time-dependent Hartree-Fock treatment of electronic and nuclear dynamics in diatomic molecules, Phys. Rev. A **83**, 063416 (2011).

[40] E. Lötstedt, T. Kato, and K. Yamanouchi, Enhanced ionization of acetylene in intense laser fields, Phys. Rev. A **85**, 041402(R) (2012).

[41] E. Lötstedt, T. Kato, and K. Yamanouchi, Intramolecular electron dynamics in the ionization of acetylene by an intense laser pulse, J. Chem. Phys. **138**, 104304 (2013).

[42] S. Roither, X. H. Xie, D. Kartashov, L. Zhang, M. Schöffler, H. L. Xu, A. Iwasaki, T. Okino, K. Yamanouchi, A. Baltuska, and M. Kitzler, High Energy Proton Ejection from Hydrocarbon Molecules Driven by Highly Efficient Field Ionization, Phys. Rev. Lett. **106**, 163001 (2011).

[43] X. H. Xie, S. Roither, M. Schöffler, H. L. Xu, S. Bubin, E. Lötstedt, S. Erattuphuza, A. Iwasaki, D. Kartashov, K. Varga, G. G. Paulus, A. Baltuška, K. Yamanouchi, and M. Kitzler, Role of proton dynamics in efficient photoionization of hydrocarbon molecules, Phys. Rev. A **89**, 023429 (2014).

[44] B. Zhang, J. M. Yuan, and Z. X. Zhao, Dynamic Core Polarization in Strong-Field Ionization of CO Molecules, Phys. Rev. Lett. **111**, 163001 (2013).

[45] S. L. Hu, Z. X. Zhao, J. Chen, and T. Y. Shi, Ionization dynamics of C_2H_2 in intense laser fields: Time-dependent Hartree-Fock approach, Phys. Rev. A **92**, 053409 (2015).

[46] J. K. Li, Z. Shu, S. L. Hu, C. R. Bi, A. P. Huang, Z. S. Xiao, J. Chen, and X. J. Liu, Dynamic interference minimum affected by permanent dipole in high-harmonic generation from CO molecules, J. Phys. B: At. Mol. Opt. Phys. **53**, 195601 (2020).

[47] H. Akagi, T. Otobe, A. Staudte, A. Shiner, F. Turner, R. Dörner, D. M. Villeneuve, and P. B. Corkum, Laser tunnel ionization from multiple orbitals in HCl, Science **325**, 1364 (2009).

[48] M. Abu-samha and L. B. Madsen, Multielectron effects in strong-field ionization of the oriented OCS molecule, Phys. Rev. A **102**, 063111 (2020).

[49] X. X. Guan, K. Bartschat, and B. I. Schneider, Breakup of the aligned H_2 molecule by XUV laser pulses: A time-dependent treatment in prolate spheroidal coordinates, Phys. Rev. A **83**, 043403 (2011).

[50] S. L. Hu, Z. X. Zhao, and T. Y. Shi, B-spline one-center method for molecular Hartree-Fock calculations, Int. J. Quan. Chem. **114**, 441 (2014).

[51] B. Zhang, J. M. Yuan, and Z. X. Zhao, DMTDHF: A full dimensional time-dependent Hartree-Fock program for diatomic molecules in strong laser fields, Comput. Phys. Commun. **194**, 84 (2015).

[52] Z. G. Sun and W. T. Yang, Communication: An exact short-time solver for the time-dependent Schrödinger equation, J. Chem. Phys. **134**, 041101 (2011).

[53] M. J. Frisch *et al.*, GAUSSIAN 09 (Gaussian Inc., Pittsburgh, 2009).

[54] P. Natalis, P. Pennetreau, L. Longton, and J. E. Collin, Ionisation energy values for the vibronic transitions from HCl $X^1\sum^+$ (v''=0) to HCl^+ ionic states $X^2\Pi$ (v'=0), J. Electron Spectrosc. Relat. Phenom. **27**, 267 (1982).

[55] A. Szabo and N. S. Ostlund, *Modern Quantum Chemistry: Introduction to Advanced Electronic Structure Theory* (Macmillan, New York, 1982).